Quantum Electronics **31** (7) 587 – 592 (2001)

INTERACTION OF LASER RADIATION WITH MATTER. LASER PLASMA

PACS numbers: 52.50.Jm; 52.38.-r; 32.80.Pj
DOI: 10.1070/QE2001v031n07ABEH002008

Metastable laser plasma

A N Tkachev, S I Yakovlenko

***Abstract*. The calculations of the multiparticle dynamics that stimulate the important stages of relaxation of an ultracold laser plasma ($N_e \sim 2 \times 10^9$ cm^{-3}, $T_e \sim 0.1$ K, $T_i \sim 10$ μK) are presented. The initial electron heating, the formation of highly excited electrons, and the confinement of electrons in a small plasma bunch are considered. Based on a previously developed analytical recombination theory of a metastable plasma, it is shown that the limiting moderation of the three-body recombination may amount to 3 – 4 orders of magnitude.**

Keywords: *laser plasma, dynamics of many-body systems, three-body recombination.*

1. Introduction

This work was initiated by papers [1, 2] on the production and investigation of an ultracold laser plasma whose lifetime turned out to be anomalously long.

In Ref. [1] the production of a laser plasma with unique parameters is reported: the charge density up to $N_e \sim 2 \times 10^9$ cm^{-3}, the electron temperature down to $T_e \sim 0.1$ K, the ion temperature down to $T_i \sim 10$ μK, and the ionisation degree ~ 0.1. The plasma was produced by two-stage photoionisation of xenon atoms in the $6s[3/2]_2$ metastable state via the $6p[5/2]_3$ state. The ionising photon energy (a wavelength of ~ 514 nm) was selected to produce upon photoionisation an electron with a low kinetic energy (0.1–1000 K). In Ref. [1], the metastable xenon atoms were obtained in a discharge, slowed down using the Zeeman deceleration technique, collected in a magneto-optical trap, and cooled by laser radiation at the $6s[3/2]_2 - 6p[5/2]_3$ transition (at a wavelength of ~ 882 nm) to a temperature of ~ 10 μK prior to ionisation.

A plasma with such temperature and density would undergo a significant recombination in a time shorter than a nanosecond. This follows both from the conventional three-body recombination theory and from the theories that take into account the nonideal plasma properties. However, the plasma lifetime observed in experiments [1, 2] was ~ 100 μs, which exceeds the three-body recombination time by many orders of magnitude. The plasma lifetime corresponded to the expansion time for heavy particles. When the density lowered by several orders of magnitude, electrons escaped from the plasma bunch. The authors of Ref. [1] called attention to an anomalously long recombination time but proposed no explanation of this effect.

An interpretation of the long lifetime of the plasma bunch was given in Ref. [3]. It was based on the concepts of a metastable overcooled plasma summarised in Refs [4 – 7]. Note that the ultracold plasma under consideration is strongly nonequilibrium in the degree of ionisation. Therefore, the theory developed in Ref. [8], which assumes ionisation and recombination to be thermodynamically equilibrium and the degree of ionisation to be defined by the Saha formula, cannot be used. As shown in Ref. [3], exchange effects (also see below) are also insignificant in the ultracold plasma under consideration, and hence the theory [9], which treats the electron gas as a Fermi liquid, cannot be applied in this case as well.

Below, we performed more detailed calculations of the initial stage of relaxation of an ultracold plasma based on classical notions. We also considered the relaxation of Rydberg states, the electron escape from the plasma bunch, and the maximum possible recombination moderation at later relaxation stages.

2. Stage of laser-induced ionisation and dynamic relaxation

2.1 On the simulation of multiparticle dynamics

An analysis of numerical simulations of multiparticle dynamics (MPD) revealed that in a time of the order of the reciprocal Langmuir frequency, a metastable state is established which is remote from the thermodynamic equilibrium in the degree of ionisation, and subsequent recombination freezes [4 – 7]. To stimulate the experimental conditions [1, 2], we performed special calculations of the MPD by the method similar described in Refs [4, 5]. As before, electrons and ions were treated as small charged spheres with diameter $d = 0.05 N_e^{-1/3}$ and the charge density was taken to be 2×10^9 cm^{-3}.

We performed calculations of two types. In the first case, we stimulated the low-temperature plasma instantaneously produced by laser-induced photoionisation. The initial conditions [the number n of electrons and ions (by 512 each)] and their coordinates were specified in the computation range (in a cube with an edge $(n/N_e)^{1/3}$ and walls specularly reflecting the particles) in accordance with the probability

A N Tkachev, S I Yakovlenko General Physics Institute, Russian Academy of Sciences, ul. Vavilova 38, 119991 Moscow, Russia

Received 7 December 2000; revision received 9 April 2001
Kvantovaya Elektronika **31** (7) 587 – 592 (2001)
Translated by E N Ragozin

density that was uniform over the cube. The electron and ion velocities were specified in accordance with the Maxwell velocity distribution with temperatures $T_{e0} = 0.1$ K for electrons and $T_{i0} = 10$ μK for ions.

In the second case we stimulated the laser-induced ionisation of neutral atoms. This allowed us to consider the cases of production of electrons with a negative total energy. The initial conditions for ions were assumed the same as in the first case. An electron was placed on each ion (the initial coordinates of the electrons and ions coincided). The electron velocities were uniformly distributed over all directions, and the specified kinetic energy differed from the ionisation energy of a given pair of particles (an 'atom') by a small value ε_0. For $\varepsilon_0 < 0$, the electron energy was below the ionisation threshold.

In both cases, we solved the Newton equations for $2n$ particles taking into account all electrostatic interactions in the system and accumulated statistics. The electron temperature was assumed to be equal to two thirds of the average electron kinetic energy. Note that the use of the classical approximation for the description of the motion of free and highly excited particles in experiments [1, 2] is fully justified [3]. The ratio between the average interparticle distance $a = (4\pi N_e/3)^{-1/3} \sim 5\times10^{-4}$ cm and the de Broglie wavelength even for $T_e \sim 0.1$ K is large, $a(m_e T_e)^{1/2}/\hbar \sim 54$ (m_e is the electron mass). For $T_e \approx 5$ K, we have $a(m_e T_e)^{1/2}/\hbar \sim 370$. For ions and atoms, $a(m_e T_e)^{1/2}/\hbar \sim 370$ for $T_i \sim 10$ μK (m_{Xe} is the xenon atom mass).

2.2 Relaxation to the metastable state

According to our results [6, 7, 10, 11], in a time of the order of half the Langmuir frequency $t \approx 0.5\omega_L^{-1}$, where $\omega_L = (4\pi e^2 N_e/m_e)^{1/2}$, electrons heat up owing to collective interactions. During this time period the mixing of phase trajectories of a system of many Coulomb particles takes place, which is characterised by the Lyapunov index $L \approx 2.4\omega_L$ [6, 7, 12, 13]. Initially the nonideality parameter $\gamma = e^2(2N_e)^{1/3} \times T_e^{-1}$ is much greater than unity. As a result of the mixing, it lowers to $\gamma_{lim} \approx 0.35 - 0.5$ for electron–ion plasmas and to $\gamma_{lim} \approx 0.64$ for charges of the equal mass.

This allowed explaining the well-known 'Langmuir paradox' [14, 15]. This paradox consists in the fact that the electron maxwellisation proceeds faster than would be expected from the kinetic theory. The Langmuir paradox cannot be explained on the basis of well-known kinetic equations. It receives an explanation [6, 7, 12, 13] as the property of dynamic mixing of the phase trajectories of a system of many Coulomb particles, resulting in the dynamic relaxation of the electron temperature in a characteristic time $\sim 0.5\omega_L^{-1}$. According to new calculations, the relaxation of an instantaneously produced ultracold plasma [1, 2] proceeds in the way as follows from our previous papers. The electron temperature T_e increases monotonically to become equal to 3.3 K in a time $\sim 0.5\omega_L^{-1} \approx 0.2$ ns, with $\gamma \approx 0.8$. Then, T_e grows slower, so that its average value amounts to 5 K, for which $\gamma \approx 0.5$ (Fig. 1).

In the ionisation to the near-threshold region ($\varepsilon_0 = -0.1$ K), the electron thermalisation stage is preceded by the stage of electron escape from the potential wells (the descending portion of the temperature curve, Fig. 2). Then, as multiparticle interactions become involved, electrons become thermalised. The behaviour of the electron temperature at a later stage is similar to the behaviour of electrons in the case of instantaneous production of an ultracold

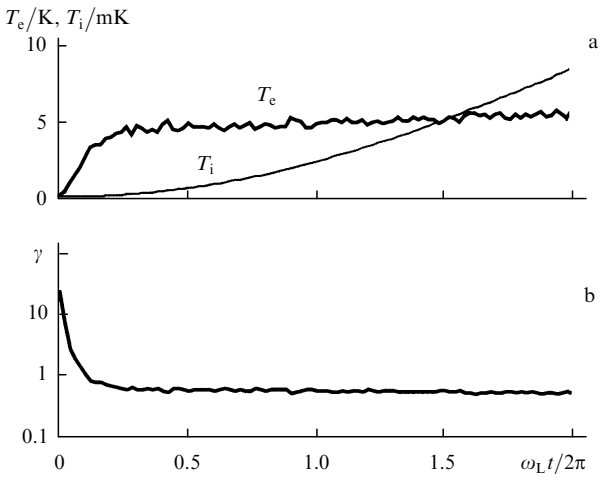

Figure 1. Time evolution of the electron and ion temperatures in the simulation of the initial relaxation stage of an instantaneously produced ultracold plasma (a) and also of the nonideality parameter $\gamma = e^2(2N_e)^{1/3}/T_e$ (b) for a number of charged particles (electrons and ions) $2n = 1024$, $N_e = 2 \times 10^9$ cm^{-3}.

plasma: in a time $\sim 0.5\omega_L^{-1} \approx 0.2$ ns, the temperature T_e reaches 3.3 K, then T_e grows slowly and its average value is 5 K. Significant departures arise for high negative energies $\varepsilon_0 < -3$ K, when electrons find themselves in the region located farther away from the threshold. This situation will be considered below.

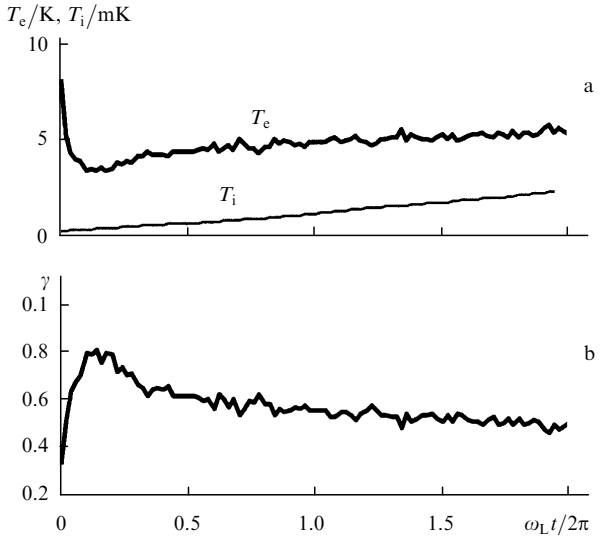

Figure 2. The same as in Fig. 1 in the simulation of ionisation for $\varepsilon_0 = -0.1$ K.

Thus, when laser-induced ionisation results in the production of electrons with a small magnitude of the total energy, the electron temperature should rise to several Kelvins in a fraction of a nanosecond. This is consistent with the data of Refs [1, 2], in which experimental results are given only for $T_e > 3.9$ K.

In Ref. [2], the ultracold plasma was subjected to the action of an alternating electric field with a frequency $f = 1 - 250$ MHz, which corresponds to the Langmuir frequency $f_L = 2\pi\omega_L$ for $N_e = 10^4 - 8\times10^8$ cm^{-3}. In this case, according to Ref. [2], the energy absorbed by the plasma regions with the resonance electron density was virtually

instantly distributed between all electrons. We believe that the heating mechanism in this case is similar to that which is responsible for the system relaxation to the metastable state. This mechanism is due to collective effects and occurs in a time $\sim 0.5\omega_L^{-1}$. Note also that in an extremely nonideal plasma, when $\gamma \approx 0.5$, the frequency of collective oscillations is 1.5–2 times lower than the Langmuir frequency, which was determined in Ref. [11]. This has to be taken into account in a more precise determination of electron density from the resonance frequency [2].

3. Electron energy distribution function

3.1 Microfield distribution

It was shown by MPD calculations [4–7] that the electron velocity distribution function in the metastable state is Maxwellian, but the electron distribution $f(\varepsilon)$ in total energy ε is essentially non-Boltzmann. In the negative energy range $\varepsilon < 0$, the distribution $f(\varepsilon)$ decays exponentially $\sim\exp(-0.32|\varepsilon|/e^2 N_e^{1/3})$. The distribution in the metastable state is therefore radically different from the Boltzmann distribution characterised by an exponential growth.

Not going into details (for more details, see Refs [4–7]), we give an expression which we usually call the *microfield distribution:*

$$f_{mf}(y) = \frac{2C}{\sqrt{\pi}} \begin{cases} \sqrt{y}\exp(-y), & y > \alpha\gamma, \\ C_3 \exp(C_1 y + C_2 y^2/2), & |y| \leqslant \alpha\gamma, \\ C_4 \exp(\beta y/\delta^{1/3}), & y < -\alpha\gamma. \end{cases} \quad (1)$$

Here, $y = \varepsilon/T_e$; $\alpha = 1.5$ and $\beta = 0.4$ are the parameters that determine the width of nonideality domain and the absolute diffusion coefficient in the negative energy range, respectively;

$$C_1(\gamma) = \frac{1}{2}\left(-1 + \frac{1}{2\alpha\gamma} + \frac{\beta}{\gamma}\right),$$

$$C_2(\gamma) = \frac{1}{2}\left(-1 + \frac{1}{2\alpha\gamma} - \frac{\beta}{\gamma}\right),$$

$$C_3 = (\alpha\gamma)^{1/2} \exp\left[-\alpha\gamma\left(1 + C_1 + \frac{1}{2}C_2\alpha\gamma\right)\right],$$

$$C_4 = (\alpha\gamma)^{1/2} \exp[\alpha\beta - \alpha\gamma(1 + 2C_1)]$$

are constants which provide the sewing conditions in the $\alpha\gamma < \varepsilon/T_e < -\alpha\gamma$ energy range; and C is the normalisation constant such that $\int f_{mf}(y)\mathrm{d}y = 1$.

The microfield distribution adequately describes all the results of numerical simulations obtained in the calculations where the time symmetry of dynamic equations was not lost. The thermodynamic functions derived on the basis of this distribution transform to the expressions of the Debye theory in the ideal plasma limit [5]. A similar distribution was also obtained here, when modelling the experimental conditions of Refs [1, 2] (Fig. 3a). In a time shorter than the reciprocal Langmuir frequency there forms a distribution in total energy close to the microfield distribution (1), which characterises the metastable state of the supercooled plasma.

3.2 Ultracold and Rydberg plasmas

An ionisation-modelling calculation revealed that different relaxation pictures are realised depending on the value of ε_0. Upon ionisation to the energy domain close enough to the threshold $\varepsilon_0 = -0.1$ K, a distribution function is formed

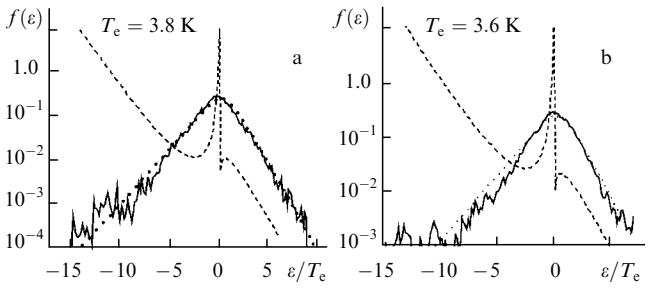

Figure 3. Electron distribution functions in total energy in the simulation of the initial relaxation stage of an instantaneously produced ultracold plasma in the metastable state with averaging over a time interval $t = (0.5 - 2.0)2\pi/\omega_L$ (see Fig. 1) (a) and in the simulation of ionisation for $\varepsilon_0 = -0.1$ K (b) (the solid lines), microfield distribution calculated by the analytical formulas of Refs [2–5] (the dotted lines) and the Boltzmann distribution (the dashed curves). The microfield and Boltzmann distributions were calculated for temperatures $T_e = 3.8$ (a) and 3.6 K (b).

which is close to that corresponding to the initial ultracold plasma conditions (Fig. 3b). If $\varepsilon_0 < -1.5\gamma T_e = -2.6$ K, the resultant distribution function is significantly different from the microfield distribution (1). It has a peak about ε_0 (Fig. 4).

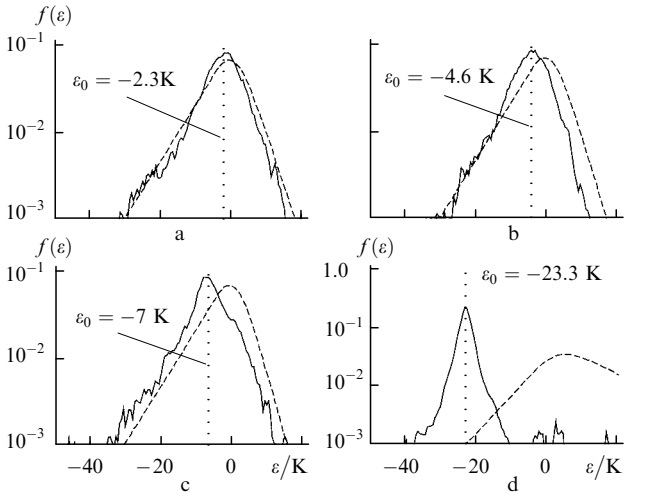

Figure 4. Electron distribution functions in total energy in the simulation of ionisation for different values of ε_0.

As mentioned above, in Refs [6, 7, 12, 13] the Lyapunov index L for an extremely nonideal plasma was shown to be equal to $\sim 15T_L^{-1} \approx 2.4\omega_L$ (where $T_L = 2\pi/\omega_L$ is the Langmuir period). Here, we will consider the question of divergence of the phase trajectories for Rydberg states. We calculate the time dependence of the distance between initially close trajectories in the coordinate and momentum spaces:

$$D_{\boldsymbol{r}} = \left\{\sum_{i=1}^{n}\left[\left(\boldsymbol{r}_{1,i} - \boldsymbol{r}_{2i}\right)^2\right]\right\}^{1/2},$$

$$D_{\boldsymbol{v}} = \left\{\sum_{i=1}^{n}\left[\left(\boldsymbol{v}_{1i} - \boldsymbol{v}_{2i}\right)^2\right]\right\}^{1/2}.$$

Here, $\boldsymbol{r}_{1i}, \boldsymbol{r}_{2i}$ is the coordinate (in μm) and $\boldsymbol{v}_{1i}, \boldsymbol{v}_{2i}$ is the velocity of the ith particle for the first and second

calculations (in km s^{-1}). The quantities D_r, D_v were calculated separately for electrons and ions (D_{re}, D_{ri} and D_{ve}, D_{vi}).

The results of calculation for $\varepsilon_0 = -7$ K are given in Fig. 5. In this case, the majority of electrons are in Rydberg states (see Fig. 4c), because the ratio between the electron orbit radius $e^2/2|\varepsilon_0| \approx 1.2\times10^{-4}$ cm and the average interparticle distance $a = (4\pi \times N_e/3)^{-1/3} \approx 5\times10^{-4}$ cm is 0.24. The time dependence of initially close trajectories is quite similar to that in the case of free electrons [6, 7]. During a time interval close to half the Langmuir period, there occurs an exponential divergence of ion and electron trajectories both in the coordinate space and in the velocity space. Then, the growth of the divergence moderates because the particle coordinates and velocities are limited. The exponent which determines the divergence of electron trajectories in both spaces is, for $n = 1024$, proportional to the Lyapunov index $L \approx 16.4T_L^{-1} \approx 2.6\omega_L$. This index is somewhat different from the index for free particles $L \approx 15T_L^{-1} \approx 2.4\omega_L$ [6, 7].

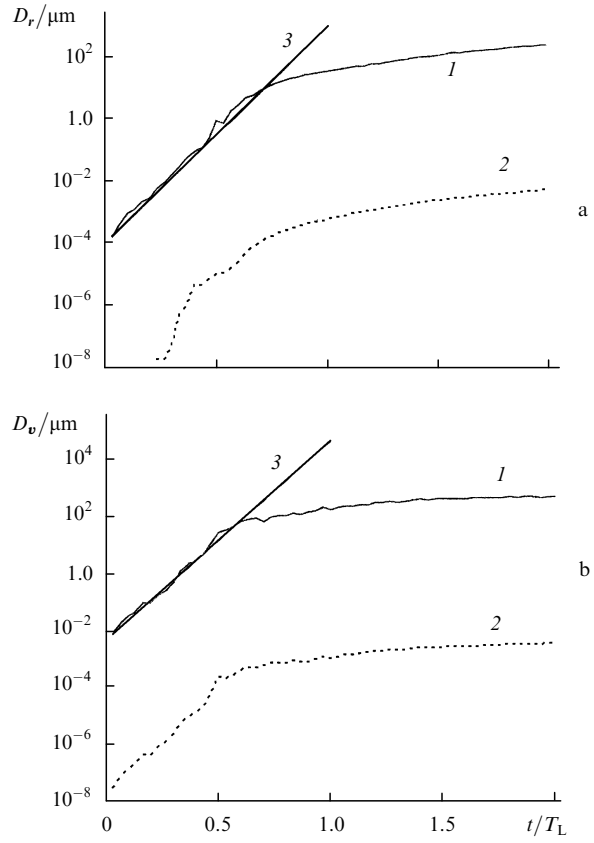

Figure 5. Distance between initially close phase trajectories of electrons D_{re}, D_{ve} (1) and ions D_{ri}, D_{vi} (2) in the coordinate (a) and velocity (b) spaces, and also dependence $\text{const}\times\exp(16.4\,t/T_L) = \text{const}\times\exp(2.6\,\omega_L t)$ (3).

An analysis of the trajectories of individual particles revealed that for $\varepsilon_0 < -1.5\gamma T_e$ electrons rotated around the nuclei nearly in circular orbits, sometimes jumping from the orbit around one ion to the orbit around another one. It is particularly remarkable that this Rydberg plasma is not destroyed by collective interactions in a time interval of the order of a Langmuir period. It is likely that the Rydberg plasma can also be metastable as is a supercooled plasma dominated by free electrons.

3.3 Modelling of a laser plasma bunch

Under the experimental conditions of Refs [1, 2], the plasma bunch dimensions were $\sim$200 μm. The bunch contained $\sim 2\times10^5$ atoms, with some fraction of the electrons escaping from the plasma volume. We performed a special simulation for estimating the effect of uncompensated charge on the plasma parameters. In the simulation of a plasma bunch, the initial coordinates of electrons and ions were prescribed inside a part of the simulation volume (a cube), namely, inside a sphere of radius $R = (4\pi N_e/3n)^{-1/3} \approx 39$ μm located at the centre of the cube (the cube edge length $l = 800$ μm). A particle reaching a cube wall was assumed to 'freeze' on it.

As would be expected, only a small fraction of electrons escapes from the sphere occupied by ions (see Fig. 6). In this case, the charge compensation is absent only at the periphery of the sphere. The computational capabilities allow us to model only a bunch of significantly smaller size than that in the experiments of Refs [1, 2]. Nevertheless, despite its small dimensions, the plasma bunch with parameters corresponding to the experiments of Refs [1, 2] confines electrons quite well: only a small fraction of them escapes from the initial sphere. In this case, the electron distribution function shifts by approximately several electron temperatures (Fig. 7) and the exponential decay in the negative energy range persists.

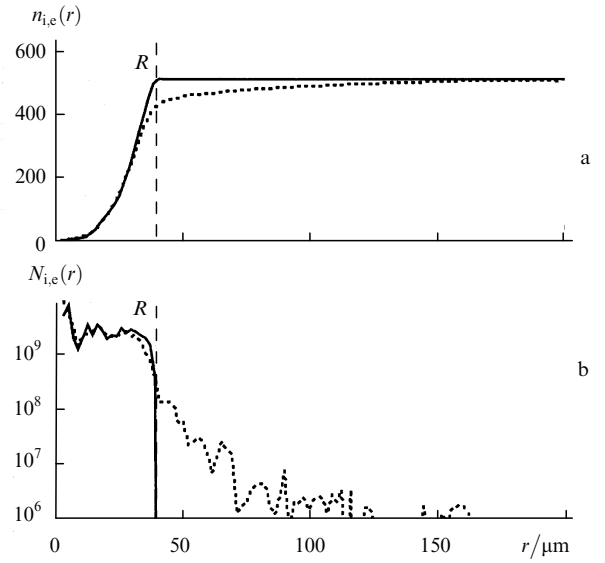

Figure 6. Distributions of the number of particles $n_{i,e}(r)$ (a) and the particle density $N_{i,e}(r)$ (b) for ions (the solid curves) and electrons (the dotted lines) in distance r to the centre of the sphere of radius R, in which their initial coordinates were prescribed, on averaging over the $7T_L < t < 8T_L$ time interval.

In connection with the above-outlined, note that an attempt was made in Ref. [16] to attribute the exponential decay of the distribution function, which was discussed in Ref. [4], to the effect of walls. This interpretation was shown to be erroneous in Ref. [17] (see also reviews [6, 7] and references therein). It goes without saying that the above results of the simulation of a 'free-hanging' plasma bunch also contradict the interpretation of Ref. [16]: the ions and the electrons of the plasma bunch do not interact with remote walls, but the electron energy distribution has an exponentially decaying slope.

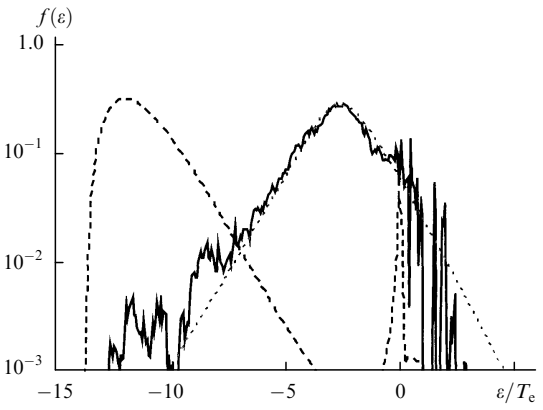

Figure 7. The same as in Fig. 3 in the case when the initial particle coordinates are located inside the sphere (compare with Fig. 6). The microfield and Boltzmann distributions were plotted for a temperature $T_e = 7.4$ K and shifted by $3T_e$ in the energy axis ε [the functions $f_B(\varepsilon/T_e - 3)$, $f_{mf}(\varepsilon/T_e - 3)$ were plotted], with averaging performed over the $7T_L < t < 8T_L$ time interval.

4. Recombination relaxation

4.1 On the recombination mechanism

The exponential decay of electron distribution in total energy in the domain of high negative energies may result in a recombination moderation in comparison with traditional notions [18, 19]. A recombination theory constructed in our earlier work (it was most comprehensively outlined in Ref. [5]) is consistent with simulation results and allows an explanation why the recombination moderation does not manifest itself under ordinary conditions. The theory is based on the assumption that diffusion in the energy axis occurs in microjumps

$$\overline{\Delta\varepsilon} \sim \left(\overline{\Delta\varepsilon^2}\right)^{1/2} \sim e^2 N_e^{1/3}.$$

This assumption imposes more stringent requirements (in comparison with the well-known ones) on the quasiclassical nature of the spectrum of bound states. For electrons with a large negative energy,

$$\varepsilon < -\varepsilon_1 = \mathrm{Ry}\left(e^2 N_e^{1/3}/2\mathrm{Ry}\right), \ \mathrm{Ry} = m_e e^4/2\hbar^2 \approx 13.6 \text{ eV}$$

and the jump $\overline{\Delta\varepsilon} \sim \left(\overline{\Delta\varepsilon^2}\right)^{1/2} \sim e^2 N_e^{1/3}$ proves to be smaller than the separation of the nearest Rydberg levels $2\mathrm{Ry}/n^3 = 2\mathrm{Ry}/(\mathrm{Ry}/\varepsilon)^{3/2}$ (n is the principal quantum number). Accordingly for $\varepsilon < \varepsilon_1$ the discreteness of the spectrum becomes significant. Relaxation in the $\varepsilon < \varepsilon_1$ energy range is dominated by pair collisions for which traditional kinetic models hold good.

The following expression was obtained for the recombination time [5]:

$$\tau_{rec}(N_e, T_e) = \tau_{rec}^{(0)} \xi. \tag{2}$$

Here, $\tau_{rec}^{(0)} \sim 0.3(m_e^{1/2} T_e^{9/2})/e^{10} N_e^2$ is the recombination time given by the conventional theory; $\xi = 1.82\delta^{5/6}\xi_1(\varepsilon_1/T_e) \times \xi_2(N_e) + 6.73\delta^{7/6}[\xi_2(N_e) - 1]$ is the correction factor; $\delta = 2e^6 N_e/T_e^2 = \gamma^3$; and

$$\xi_1(z) = \left(e^z/4z^{5/2}\right) \int_z^\infty dy\, y^{3/2} e^{-y} \times \left[1 + 6y + 0.75y^2 + \left(\pi y^3/16\right)\right]^{1/2}; \tag{3}$$

$$\xi_2(N_e) = \exp[-0.4(\varepsilon_1 - 1.5e^2 N_e^{1/3})/2^{1/2} e^2 N_e^{1/3}].$$

According to our theory, a significant moderation of plasma recombination takes place when $[\varepsilon_1/1.5e^2(2N_e)^{1/3}] \gg 1$, which can be written as $(N_e^{cr}/N_e)^{1/9} \gg 1$, where $N_e^{cr} \equiv (\mathrm{Ry}/27e^2)^3 \approx 4.3\times10^{19}$ cm^{-3}. For instance, for $N_e = 2\times10^9$ cm^{-3} we have $(N_e^{cr}/N_e)^{1/9} = 14$.

Note that the validity of the traditional recombination theory is bounded by the condition $\gamma^3 \ll 1$ (see below). The smallness of electron temperature in comparison with the ionisation energy suffices for the validity of the diffusion approximation employed both in the traditional [18, 19] and our theories.

4.2 Comparison with experiments

Expression (2) yields results close to those of the conventional three-body recombination theory in the range of not-too-low plasma temperatures and densities ($\xi \sim 1$ for $T_e > 0.03$ eV ≈ 350 K, $N_e > 10^{10}$ cm^{-3}). Accordingly, the emphasis previously was on the feasibility of producing a strongly supercooled ion–ion plasma where quantum effects were of minor importance. The range of parameters of an electron–ion plasma where recombination freezing is significant seemed hard to realise in experiments.

In addition, for the experimental observation of the metastable plasma state, conditions are required whereby the external stochastisation of the system of Coulomb particles is weak. In particular, collisions with neutral particles should be infrequent. This leads to the requirement that the degree of ionisation of the plasma should be high. Also possible are other causes for stochastic effects, which are hard to take into consideration.

We estimate the characteristic recombination time for the experimental conditions of Refs [1, 2]. For $T_e = 5$ K and $N_e = 2\times10^9$ cm^{-3}, expression (2) yields a significant recombination moderation in comparison with the conventional theory: $\xi = 2.4\times10^3$. In this case, the characteristic recombination time τ_{rec} given by our theory is 60 μs. For $T_e = 5$ K and $N_e = 10^9$ cm^{-3}, we have $\xi = 2.5\times10^3$, $\tau_{rec} = 210$ μs. This is consistent with the results of experiments of Refs [1, 2], where an ultracold plasma persisted for ~ 100 μs. Radiative recombination can be neglected under these conditions; its time is several seconds.

4.3 Recombination of an extremely cold plasma

Proceeding from the limiting value $\gamma_{lim} \approx 0.5$, it is possible to predict the ultimately low temperature of the metastable state

$$T_e^{met}(N_e) \approx e^2(2N_e)^{1/3}/\gamma_{lim} \approx (N_e 10^9 \mathrm{cm}^3)^{1/3} 4.2 \text{ K}, \tag{4}$$

which can be obtained in the ionisation of atoms to the near-threshold region $|\varepsilon_0| \ll T_e^{met}$. Given this charge density, the electron temperature of the plasma residing in the metastable state cannot be lower than $T_e^{met}(N_e)$. In an extremely cold metastable plasma, the recombination time is therefore determined by the density of charged particles (Fig. 8).

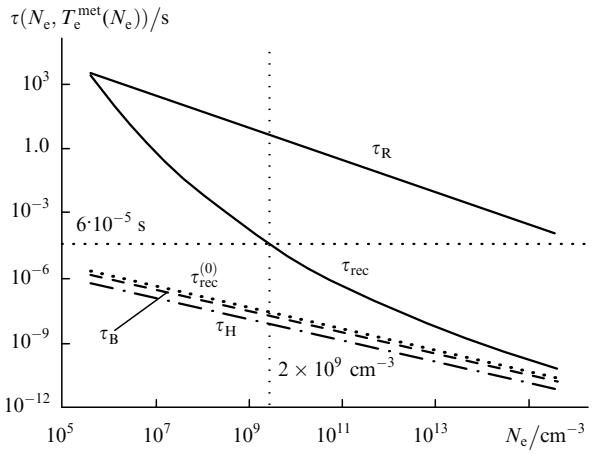

Figure 8. Density dependence of the characteristic recombination time of an extremely cold metastable plasma $\tau(N_e, T_e^{met}(N_e))$ by our theory [τ_{rec}, formula (2)], by the conventional theory [$\tau_{rec}^{(0)}$, formula (9)], taking into account the plasma nonideality [τ_B, formula (5)] and the plasma density limitation [τ_H, formula (6)], and by the theory of radiative recombination [τ_R, formula (7)].

There are several papers which take into account the departures from the traditional theory arising from plasma nonideality [20] and the effects of charge density [21]. From Ref. [20] there follows an expression for the characteristic recombination time

$$\tau_B(N_e, T_e) = \frac{T_e^{3/2} m_e^{1/2}}{5.231 e^4 \Lambda \left\{1+\exp\left[-(4\pi/6)[\gamma(N_e, T_e)\times 0.543]^3\right]\right\}[1+\gamma(N_e, T_e)/2^{1/3}]^{1/2}}. \quad (5)$$

Here, we have corrected several numerical inaccuracies of the formulas of Ref. [20].

The following expression follows from Ref. [21] for the characteristic recombination time:

$$\tau_H(N_e, T_e) = \max\{\tau_1, \tau_2\}, \quad (6)$$

where $\tau_2 = \left[N_e^2 (\mathrm{Ry}/T_e)^{4.5} \times 2.156\times10^{31}\ \mathrm{cm}^6\ \mathrm{c}^{-1}\right]^{-1}$ and $\tau_2 = [N_e^{5/6} \times \mathrm{Ry}/T_e \times 3.528\times10^4\ \mathrm{cm}^{5/2}\ \mathrm{s}^{-1}$. The following simple expression [22] was taken for the radiative recombination time in Fig. 8:

$$\tau_R(N_e, T_e) = [N_e T_e \times 2.7\times10^{-13}\ \mathrm{cm}^3\ \mathrm{c\ eV}^{-1})]^{-1}. \quad (7)$$

One can see from Fig. 8 that the radiative recombination time in an extremely cold plasma is, up to $N_e \sim 10^6$ cm^{-3}, much longer than the recombination time defined by our theory. For an extremely cold plasma, expressions (5) and (6) yield values close to the results of the traditional theory, which is natural because $\gamma_{lim}^3 \approx 0.125 \ll 1$.

5. Conclusions

Thus, there are grounds to believe that an abnormally slow relaxation (i.e., metastability) of an ultracold plasma took place in the experiments of Refs [1, 2]. Within the framework of the conventional theory, in less than a microsecond the plasma should have recombined by more than 10 % and the electron temperature have increased several times compared to $T_e^{met}(N_e)$. This should be accompanied by an additional flow of electrons from the plasma bunch which, however, was not observed in the experiments of Refs [1, 2]. The question of the plasma bunch expansion taking into account the electron heating invites additional investigation.

Acknowledgements. The authors are grateful to T Killian for discussing issues related to the experiments of Refs [1, 2] via e-mail.

References

1. Killian T C, Kulin S, Bergeson S D, Orozco L A, Orzel C, Rolston S L *Phys. Rev. Lett.* **83** 4776 (1999)
2. Kulin S, Killian T C, Bergeson S D, Rolston S L *Phys. Rev. Lett.* **85** 318 (2000)
3. Tkachev A N, Yakovlenko S I *Kvantovaya Elektron.* **30** 1077 (2000) [*Quantum Electron.* **30** 1077 (2000)]
4. Maiorov S A, Tkachev A N, Yakovlenko S I *Usp. Fiz. Nauk* **164** 297 (1994) [*Phys. Uspekhi* **37** 279 (1994)]
5. Maiorov S A, Tkachev A N, Yakovlenko S I *Phys. Scr.* **51** 498 (1995)
6. Tkachev A N, Yakovlenko S I *Izv. Vyssh. Uchebn. Zaved. Ser. Fiz.* **41** (1) 47 (1988)
7. Yakovlenko S I *Phys. Vibr.* **6** 267 (1998)
8. Norman G E *Khim. Fiz.* **18** (7) 78 (1999)
9. Manykin E A, Ozhovan M I, Poluektov P P *Khim. Fiz.* **18** (7) 87 (1999)
10. Tkachev A N, Yakovlenko S I *Pis'ma Zh. Tekh. Fiz.* **21** (22) 90 (1995)
11. Tkachev A N, Yakovlenko S I *Zh. Tekh. Fiz.* **67** (8) 42 (1997)
12. Tkachev A N, Yakovlenko S I *Pis'ma Zh. Tekh. Fiz.* **23** (17) 68 (1997)
13. Tkachev A N, Yakovlenko S I *Dokl. Ross. Akad. Nauk* **359** 765 (1998)
14. Langmuir I *Phys. Rev.* **28** 585 (1925)
15. Forester A T *Large Ion Beams* (New York: Wiley, 1988)
16. Ignatov A M, Korotchenko A I, Makarov V P, Rukhadze A A, Samokhin A A *Usp. Fiz. Nauk* **165** 113 (1995) [*Phys. Uspekhi* **38** 109 (1995)]
17. Maiorov S A, Tkachev A N, Yakovlenko S I *Usp. Fiz. Nauk* **165** 117 (1995) [*Phys. Uspekhi* **38** 113 (1995)]
18. Gurevich A V *Geomagn. Aeronom.* **4** (1) 3 (1964)
19. Gurevich A V, Pitaevskii L P Zh. *Eksp. Teor. Fiz.* **46** 1281 (1964)
20. Biberman L M, Vorob'ev V S, Yakubov I T *Dokl. Akad. Nauk SSSR* **96** 576 (1986)
21. Hahn Y *Phys. Lett. A* **231** 82 (1977)
22. Raizer Yu P *Fizika Gazovogo Razryada* (The Physics of a Gas Discharge) (Moscow: Nauka, 1992)